Supporting Information

Mesoporous Co-O-C Nanosheets for Electrochemical Production of Hydrogen Peroxide in Acidic Medium

Lingyan Jing[#ab], Qiang Tian[#ab], Panpan Su[a], Haitao Li[a], Yao Zheng[c], Cheng Tang[*c], Jian Liu[*abd]

[a] State Key Laboratory of Catalysis, Dalian Institute of Chemical Physics, Chinese Academy of Sciences, 457 Zhongshan Road, Dalian 116023, China

[b] University of Chinese Academy of Sciences, Beijing 100049, China.

[c] School of Chemical Engineering and Advanced Materials, The University of Adelaide, Adelaide, SA 5005, Australia

[d] DICP-Surrey Joint Centre for Future Materials, Department of Chemical and Process Engineering, University of Surrey, Guildford, Surrey GU2 7XH, UK

*Corresponding Author:

E-mail: cheng.tang@adelaide.edu.au

E-mail: jianliu@dicp.ac.cn; jian.liu@surrey.ac.uk

Supplementary Tables

Table S1. Summary of C, N and O contents in different samples based on the XPS measurements.

Sample	Atomic content (at %)				Relative content (%)	
	C	O	N	Co	C=O	C–O
MesoC-Co	85.74	13.27	0.99	/	28.74	71.26
MicroC-Co	86.99	10.57	2.44	/	27.54	72.46
GO-Co	87.88	9.13	2.83	0.16	23.59	76.41

Table S2. Comparison of electrochemical H_2O_2 production via $2e^-$ ORR in acid.

Catalyst	Electrolyte	Onset potential (V_{RHE})	Disk current density @0.3 V_{RHE} / mA cm^{-2}	Selectivity (%@V_{RHE})	Stability test	Ref.
MesoC-Co	0.1 M $HClO_4$	0.73	–2.4	> 80 @ (0.3–0.6)	24 h	This work
Pt-Hg/C	0.1 M $HClO_4$	0.6	–0.53	> 90 @(0.3–0.5)	8000 cycles	1
Au-Pd/C	0.1 M $HClO_4$	0.4	–0.5	90 @(0.1)	/	2
Co-N-C	0.5 M H_2SO_4	0.7	–2.7	80 @(0.1)	6 h	3
Co-NC	0.1 M $HClO_4$	0.75	–2.5	> 90 @(0.6)	10 h	4
Pt/HSC	0.1 M $HClO_4$	0.7	–1.0	94 @(0.5)	6 h	5
CoN@CNTs	0.1 M $HClO_4$	0.65	–2.5	> 95 @(0.3–0.6)	12 h	6
$CoSe_2$	0.05 M H_2SO_4	0.7	–3.0	80 @(0.4)	4.2 h	7
$MoTe_2$	0.5 M H_2SO_4	0.56	–0.9	80 @(0.3)	5000 cycles	8
MNC	0.1 M $HClO_4$	0.5	–1.0	65.2 @(0.1)	6 h	9
C(Pt)/C	1 M $HClO_4$	0.7	–1.0	41 @(0.1)	/	10
Pt_1/TiN	0.1 M $HClO_4$	0.56	–1.0	55 @(0.4)	6 h	11

Supplementary Figures

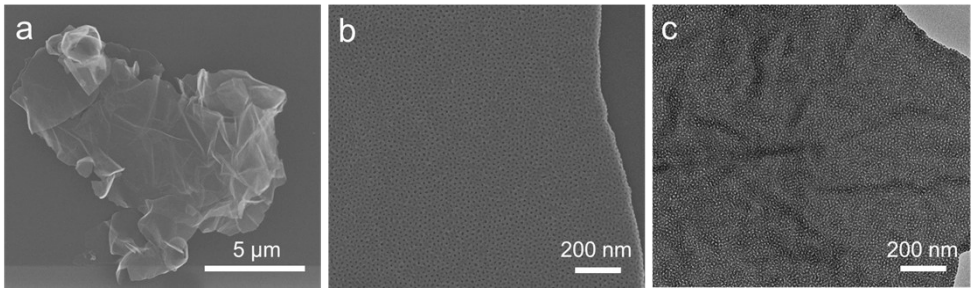

Figure S1. (a, b) SEM images and (c) TEM image of GO@MRF.

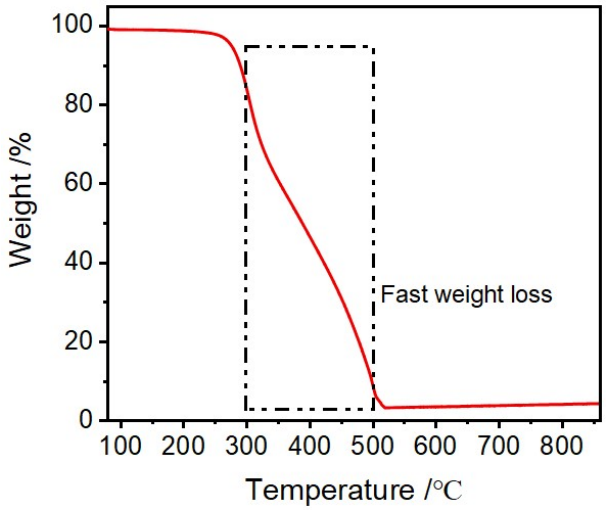

Figure S2. The thermal gravimetric analysis of GO@MRF under N_2 atmosphere.

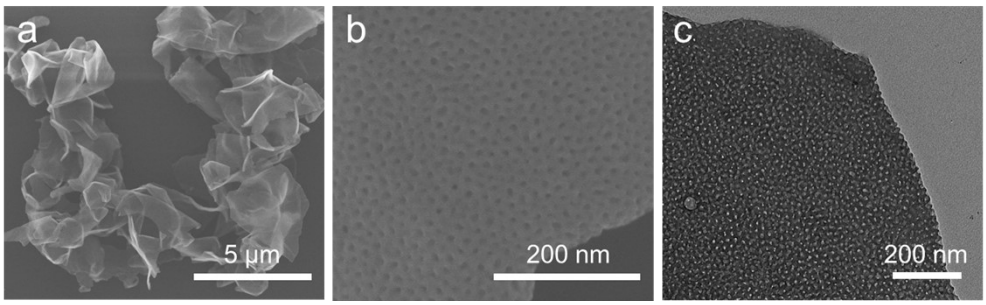

Figure S3. (a, b) SEM images and (c) TEM image of MesoC.

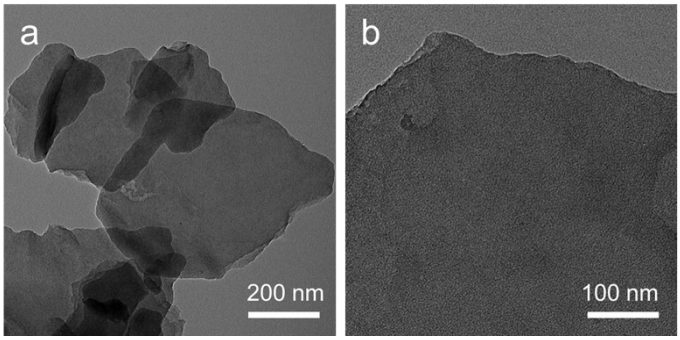

Figure S4. TEM images of MicroC-Co.

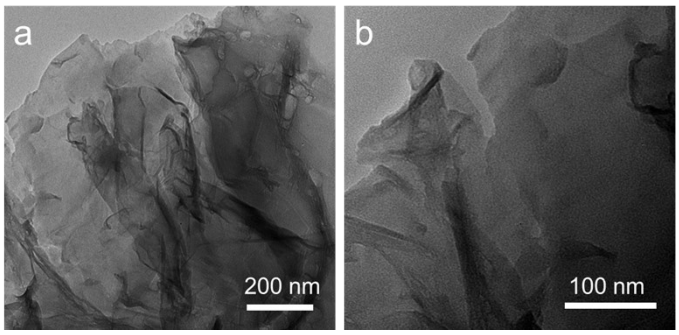

Figure S5. TEM images of GO-Co.

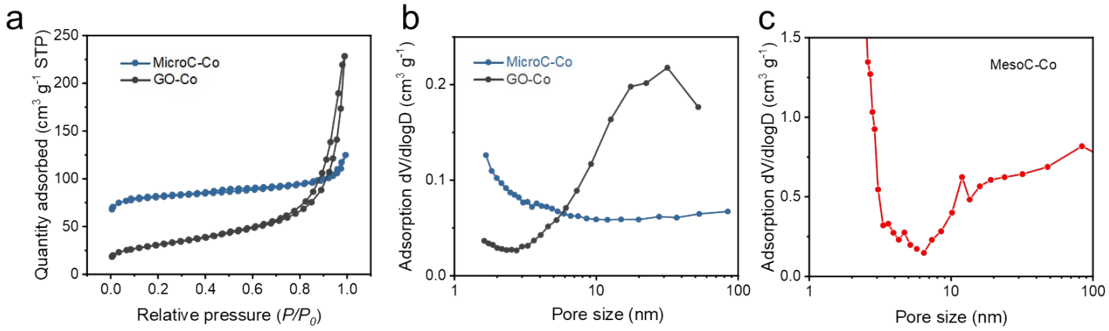

Figure S6. (a) Nitrogen adsorption-desorption isotherms and (b) corresponding pore size distributions of MicroC-Co and GO-Co samples. (c) Pore size distribution of MesoC-Co.

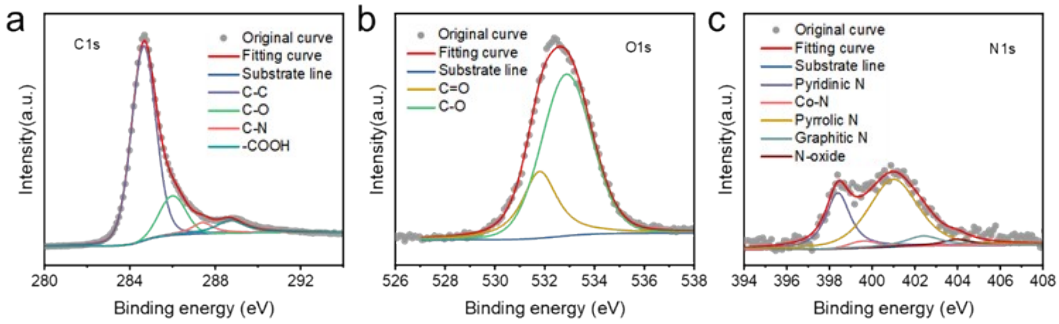

Figure S7. High-resolution (a) C 1s, (b) O 1s and (c) N 1s XPS spectra of MicroC-Co.

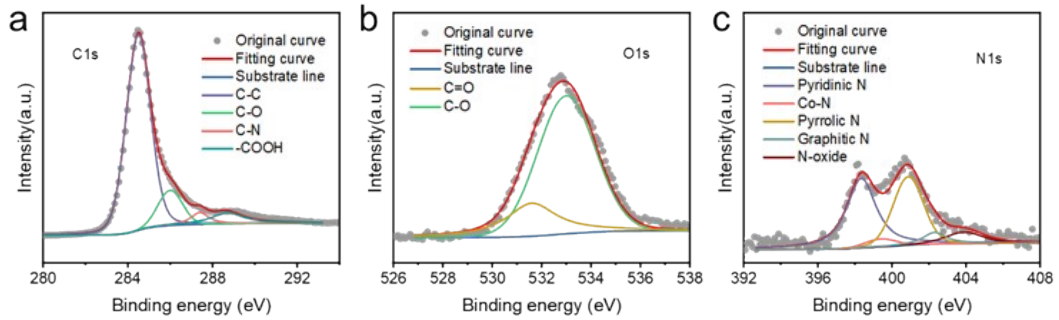

Figure S8. High-resolution (a) C 1s, (b) O 1s and (c) N 1s XPS spectra of GO-Co.

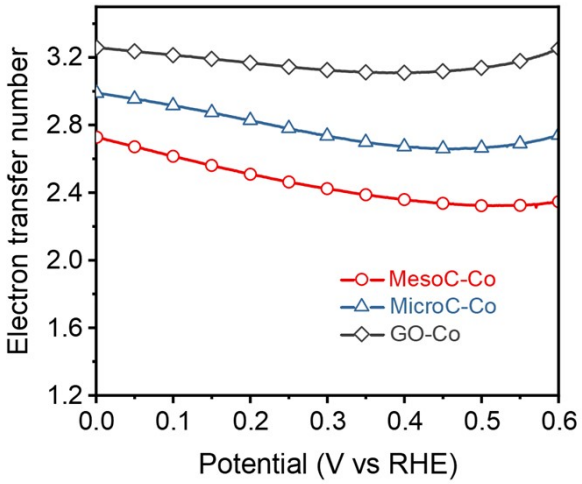

Figure S9. Calculated ORR electron transfer number for three samples in O_2-saturated 0.10 M $HClO_4$.

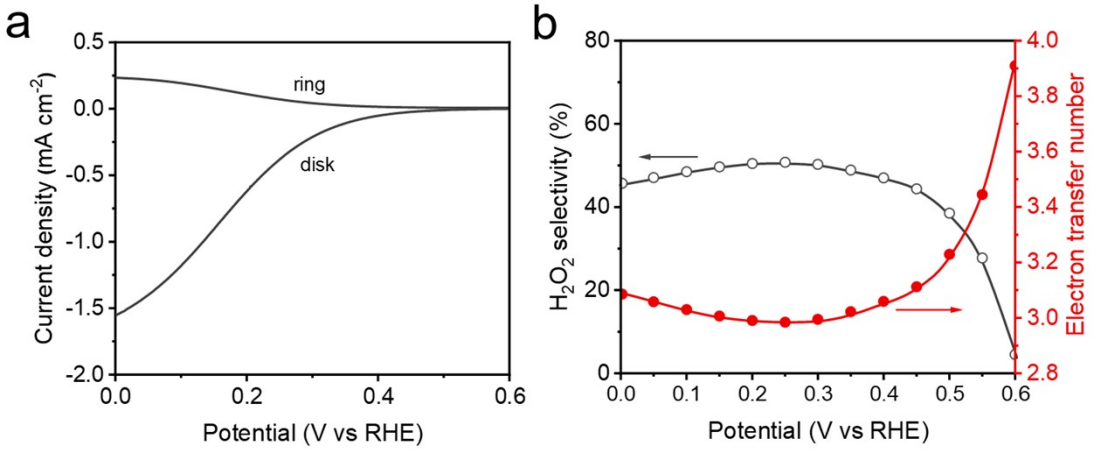

Figure S10. (a) Linear sweep voltammetry (LSV) curves of MesoC in 0.10 M $HClO_4$ and (b) its corresponding H_2O_2 selectivity and electron transfer number during the potential sweep.

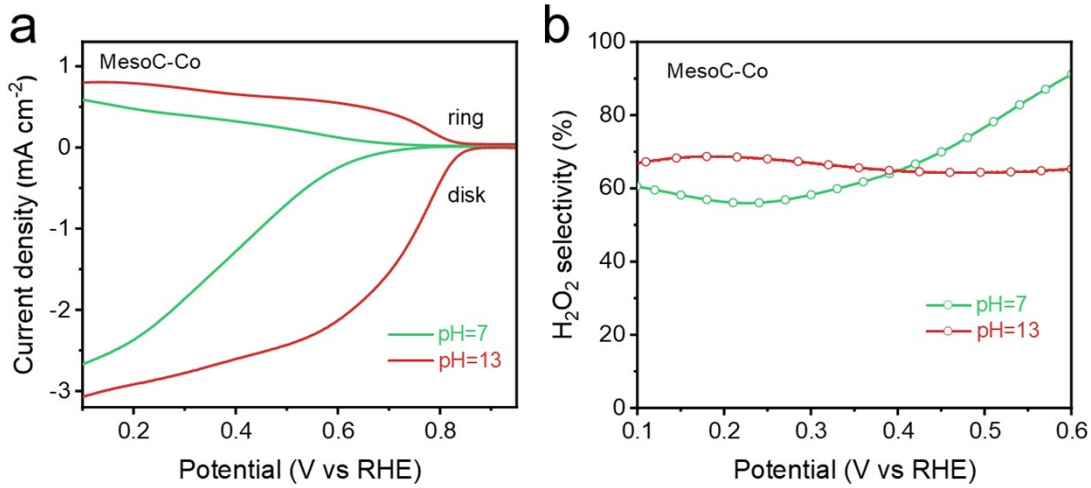

Figure S11. (a) LSV curves of MesoC-Co in O_2-saturated electrolytes of different pH values. (b) Calculated H_2O_2 selectivity as a function of applied potential.

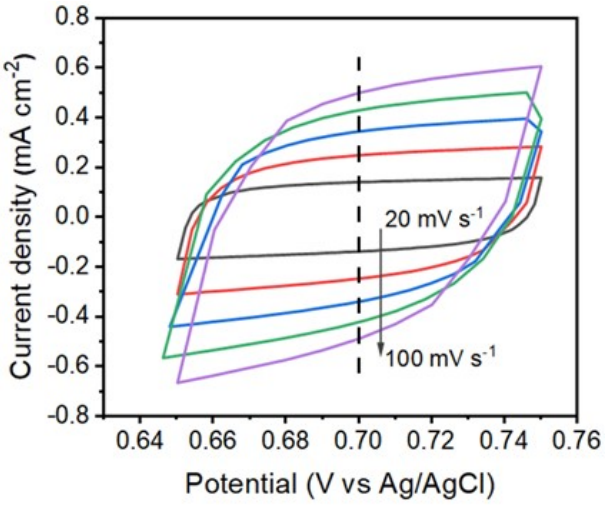

Figure S12. (a) Cyclic voltammogram (CV) curves of MesoC-Co in the double layer region at scan rates of 20, 40, 60, 80, and 100 mV s^{-1} in N_2-sautrated 0.1 M $HClO_4$ (pH = 1) aqueous electrolyte.

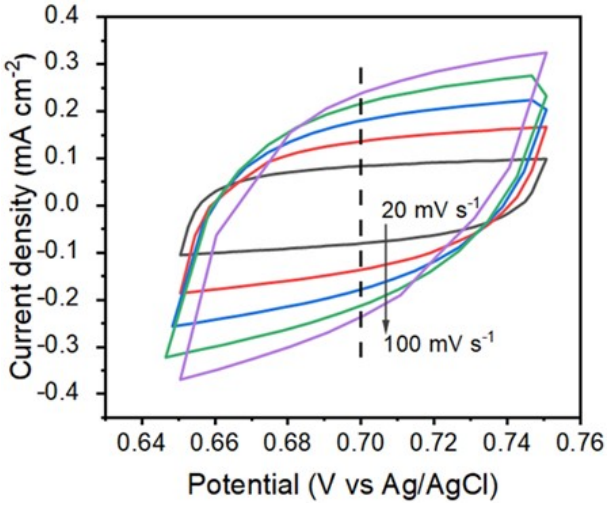

Figure S13. (a) CV curves of MicroC-Co in the double layer region at scan rates of 20, 40, 60, 80, and 100 mV s^{-1} in N_2-sautrated 0.1 M $HClO_4$ (pH = 1) aqueous electrolyte.

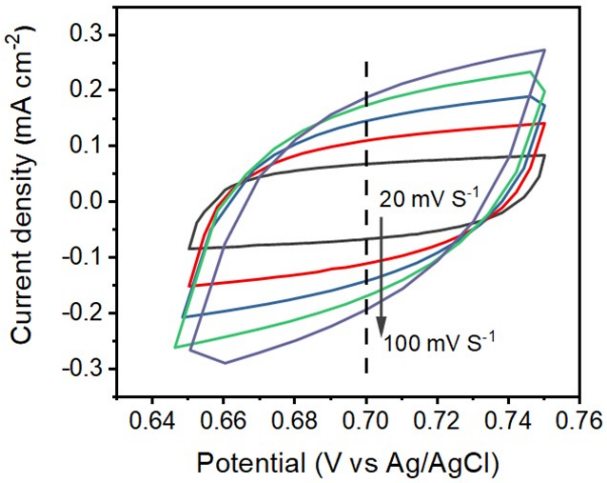

Figure S14. (a) CV curves of GO-Co in the double layer region at scan rates of 20, 40, 60, 80, and 100 mV s^{-1} in N_2-sautrated 0.1 M $HClO_4$ (pH = 1) aqueous electrolyte.

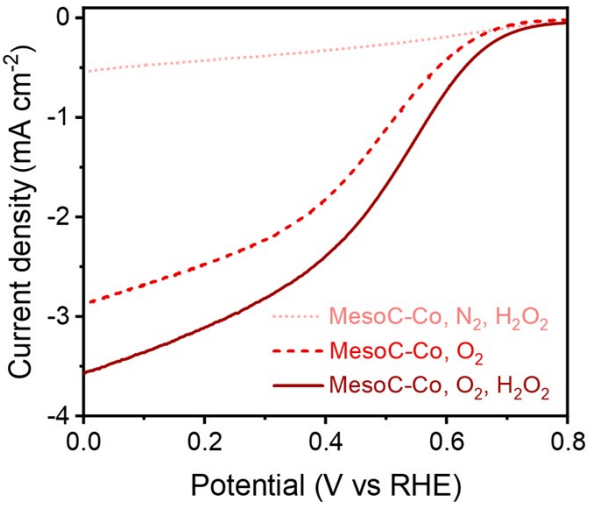

Figure S15. LSV curves of MesoC-Co sample in 0.10 M $HClO_4$ with different conditions, including O_2-saturated electrolyte without H_2O_2, O_2-saturated electrolyte containing 10 mM H_2O_2, and N_2-saturated electrolyte containing 10 mM H_2O_2.

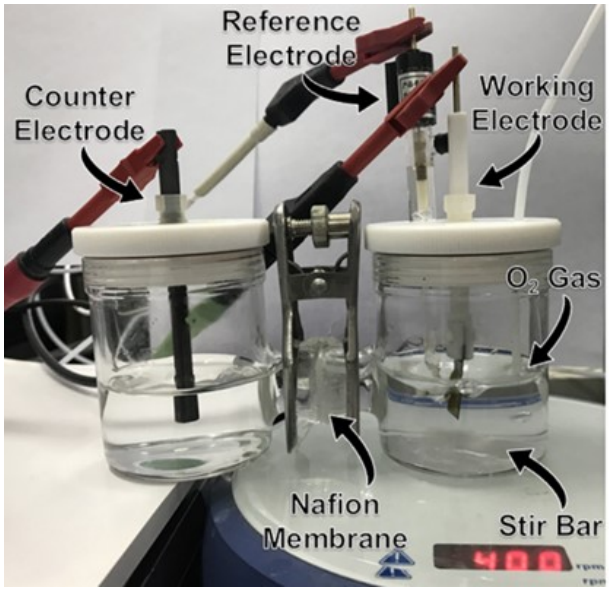

Figure S16. Digital photograph of the two-compartment three-electrode H-cell setup used for the electrochemical synthesis of H_2O_2.

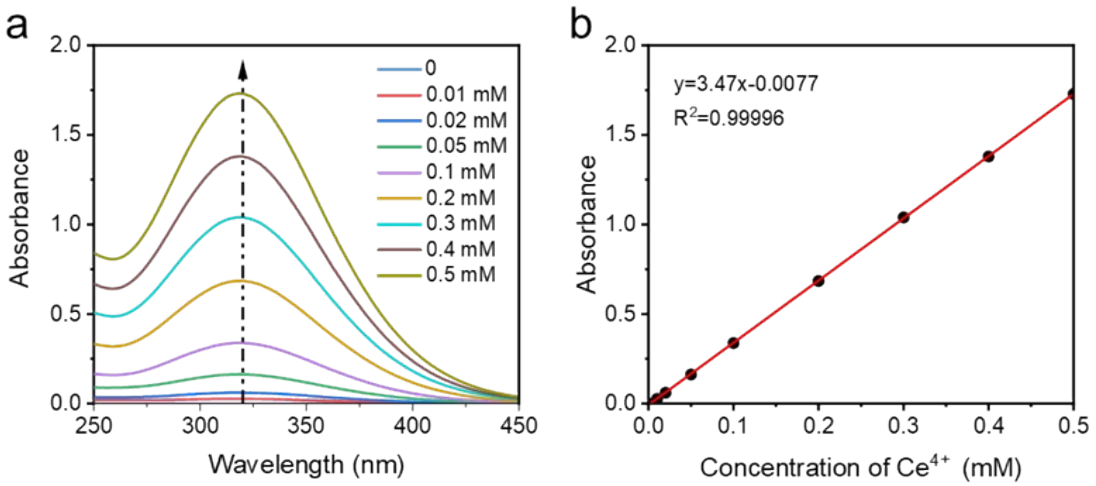

Figure S17. (a) UV-Vis absorption spectra of Ce^{4+} solution with various concentrations and (b) its corresponding standard curve.

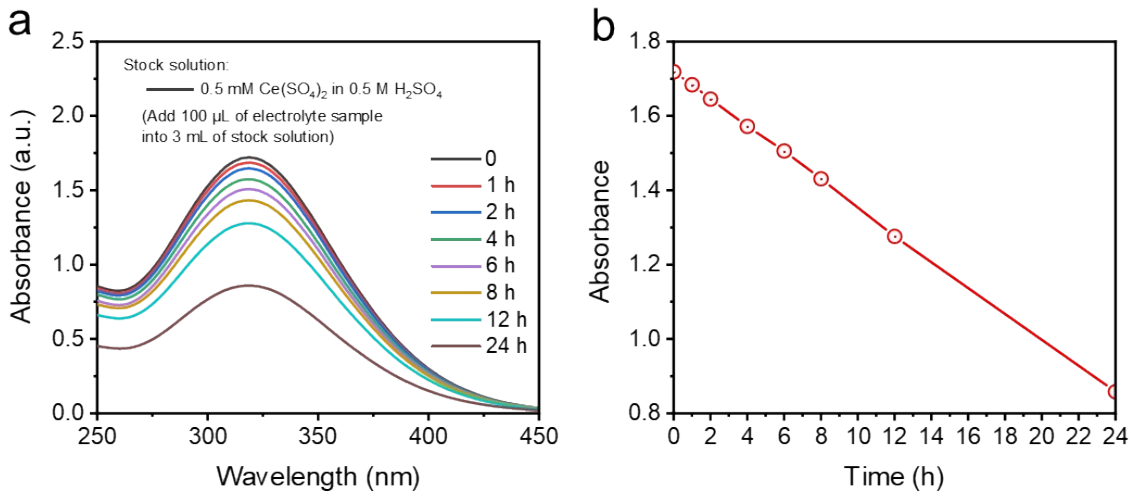

Figure S18. (a) UV-Vis absorption spectra of the quantitatively diluted small aliquot of electrolyte solution sampled from the working electrode compartment at various time points during the stability test. (b) Plot of the absorbance change at wavelength of 320 nm versus reaction time of H_2O_2 generation.

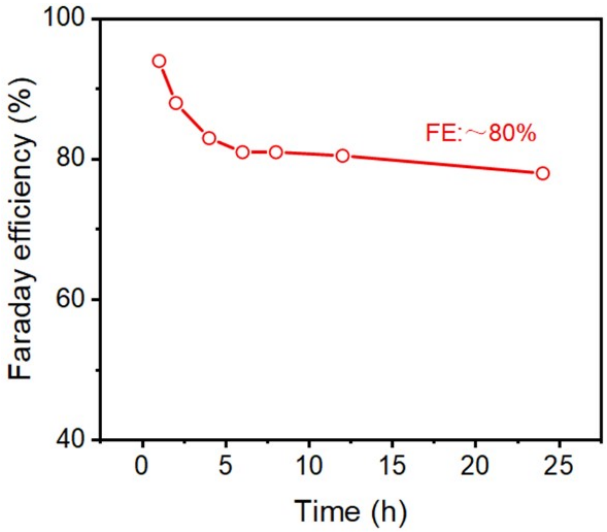

Figure S19. The calculated H_2O_2 Faraday efficiency (FE) of MesoC-Co as a function of time.

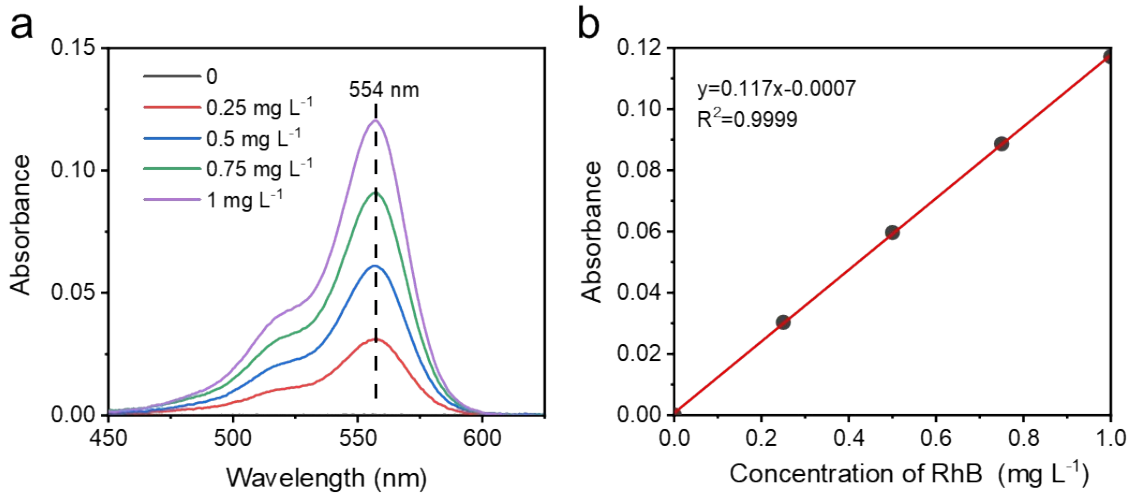

Figure S20. (a) UV-Vis absorption spectra of RhB standard solutions with various concentrations in acidified 0.5 M Na_2SO_4 solution (pH = 2.85) and (b) its corresponding standard curve.

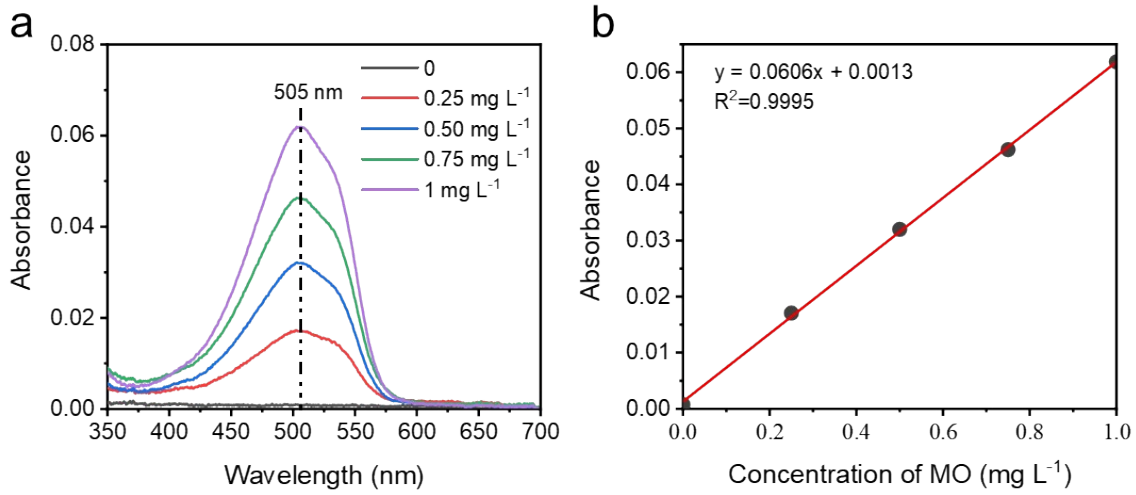

Figure S21. (a) UV-Vis absorption spectra of MO standard solutions with various concentrations in acidified 0.5 M Na_2SO_4 solution (pH = 2.85) and (b) its corresponding standard curve.

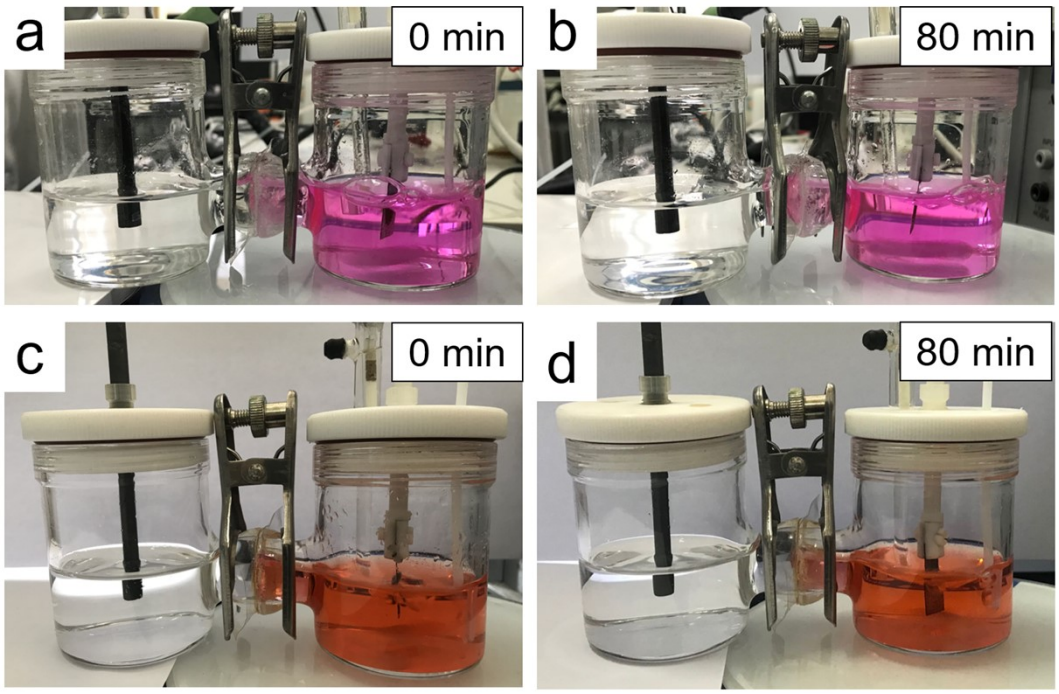

Figure S22. The photographs track the color changes of the electrolyte solutions before and after 80 min without electricity inputs. (a, b) RhB solution, (c, d) MO solution.

Supplementary References

1. S. Siahrostami, A. Verdaguer-Casadevall, M. Karamad, D. Deiana, P. Malacrida, B. Wickman, M. Escudero-Escribano, E. A. Paoli, R. Frydendal and T. W. Hansen, *Nat. Mater.*, 2013, **12**, 1137-1143.

2. J. S. Jirkovský, I. Panas, E. Ahlberg, M. Halasa, S. Romani and D. J. Schiffrin, *J. Am. Chem. Soc.*, 2011, **133**, 19432-19441.

3. Y. Sun, L. Silvioli, N. R. Sahraie, W. Ju, J. Li, A. Zitolo, S. Li, A. Bagger, L. Arnarson and X. Wang, *J. Am. Chem. Soc.*, 2019, **141**, 12372-12381.

4. J. Gao, H. b. Yang, X. Huang, S. F. Hung, W. Cai, C. Jia, S. Miao, H. M. Chen, X. Yang, Y. Huang, T. Zhang and B. Liu, *Chem*, 2020, **6**, 658-674.

5. C. H. Choi, M. Kim, H. C. Kwon, S. J. Cho, S. Yun, H. T. Kim, K. J. Mayrhofer, H. Kim and M. Choi, *Nat. Commun.*, 2016, **7**, 10922.

6. Q. Zhang, X. Tan, N. M. Bedford, Z. Han, L. Thomsen, S. Smith, R. Amal and X. Lu, *Nat. Commun.*, 2020, **11**, 4181.

7. H. Sheng, A. N. Janes, R. D. Ross, D. Kaiman, J. Huang, B. Song, J. Schmidt and S. Jin, *Energy Environ. Sci.*, 2020, **13**, 4189-4203.

8. X. Zhao, Y. Wang, Y. Da, X. Wang, T. Wang, M. Xu, X. He, W. Zhou, Y. Li and J. N. Coleman, *Natl. Sci. Rev.*, 2020, **7**, 1360-1366.

9. T. P. Fellinger, F. D. R. Hasché, P. Strasser and M. Antonietti, *J. Am. Chem. Soc.*, 2012, **134**, 4072-4075.

10. C. H. Choi, H. C. Kwon, S. Yook, H. Shin, H. Kim and M. Choi, *J. Phys. Chem. C*, 2014, **118**, 30063-30070.

11. S. Yang, J. Kim, Y. J. Tak, A. Soon and H. Lee, *Angew. Chem. Int. Ed.*, 2016, **55**, 2058-2062.